SETI Pulse Detection Algorithm: Analysis of False-Alarm Rates

B. K. Levitt
Communications Systems Research Section

This report extends some earlier work by the Search for Extraterrestrial Intelligence (SETI) Science Working Group (SWG) on the derivation of spectrum analyzer thresholds for a pulse detection algorithm based on an analysis of false-alarm rates. The algorithm previously analyzed was intended to detect a finite sequence of i periodically spaced pulses that did not necessarily occupy the entire observation interval. This algorithm would recognize the presence of such a signal only if all i-received pulse powers exceeded a threshold T(i): these thresholds were selected to achieve a desired false-alarm rate, independent of i. To simplify the analysis, it was assumed that the pulses were synchronous with the spectrum sample times.

This analysis extends the earlier effort to include infinite and/or asynchronous pulse trains. Furthermore, to decrease the possibility of missing an ETI signal, the algorithm has been modified to detect a pulse train even if some of the received pulse powers fall below the threshold. The analysis employs geometrical arguments that make it conceptually easy to incorporate boundary conditions imposed on the derivation of the false-alarm rates. While the exact results can be somewhat complex, simple closed form approximations are derived that produce a negligible loss of accuracy.

I. Introduction

Just as a flashing light commands more attention than constant illumination for the same average power, a sequence of pulses is a more likely extraterrestrial intelligence (ETI) beacon than a continuous wave (CW) signal. Oliver has shown that there is a signal-to-noise-ratio (SNR) advantage in detecting pulse trains over CW signals (Ref. 1, p. 39). Furthermore, pulsed signals are less likely to be confused with natural phenomena. So the pulse detection algorithm is an important element of SETI.

In both the sky and target survey modes of operation, the received signals will be processed by a multichannel spectrum analyzer (MCSA), which generates a temporal sequence of observed powers in a large number of contiguous frequency bins. For real-time operation, it would be impractical to apply an ETI detection algorithm directly to this frequency-time matrix of analog powers. So each power is compared with a set of thresholds to create a reduced observation space of soft-quantized powers: the algorithms then search this simplified space for signals of interest.

Suppose we are interested in detecting a sequence of narrowband periodic pulses. For simplicity, assume we do not have to compensate for frequency drifts, so that if one of the pulses is observed in a particular frequency bin, subsequent pulses will be observed in the same bin: the analysis that follows will isolate the operation of a pulse detection algorithm on a single representative frequency cell corresponding to a particular MCSA resolution.

The detection problem is complicated by the largely unknown nature of the signal of interest. The only certainty under our hypothesis is that the signal is periodic. We do not have a priori knowledge of the received power, center frequency, bandwidth, pulse duration, period, or time of occurrence of the first observed pulse, nor do we have statistical distributions for these parameters. We also do not know the likelihood of observing an ETI pulse train, although the presumption is that such an event is extremely rare. Because of this last consideration, we tend to select an algorithm that ensures tolerable false-alarm rates, without regard for the probability of missing an ETI event: this paper adheres to that premise.

The analysis that follows will focus on the false-alarm rate for a particular pulse detection algorithm that searches for patterns of i periodically spaced hits in a threshold detected record of finite duration for a given frequency bin, where i is an unknown variable. We will assume that the duration of each pulse is no larger than the inverse resolution bandwidth, which is the time required to generate each spectral measurement: so each pulse affects at most two adjacent temporal observations if it starts in the first and ends in the second, and if the pulse duration is small enough, most of the power will impact a single time cell. In analyzing false-alarm rates, the desired signal is absent: it is only the internal system noise that can cause a particular measurement to exceed the operating threshold. If the detection algorithm demands that all i hypothetically observed pulses cause the corresponding temporal measurements to exceed a selected threshold $T(i)$, the likelihood of this occurring due to noise alone decreases with i. Conversely, if we want to maintain a desired false-alarm rate independent of i, we must employ a sequence of thresholds $\{T(i)\}$, where $T(i)$ decreases with i. This last approach was adopted by Cullers based on a preliminary false-alarm analysis for "regular" (periodic) pulses (Ref. 1, pp. 12-19).

This paper extends that earlier work, and the initial thinking that went into it provided a welcome opportunity for Cullers and me to collaborate in the evolution of the SETI pulse detection algorithm. In the course of this effort, we agreed on some useful terminology. In particular, a "finite" pulse train refers to a signal of limited duration that may begin and/or end within a given observation interval, whereas an "infinite" pulse sequence is assumed to extend indefinitely before and after that interval. For computational convenience it was useful to introduce the mathematical artifice of a "synchronous" pulse train wherein each received pulse coincides with a spectral time cell. Of course, the probability of this serendipitous occurrence is strictly zero, and realistically we should consider the situation in which the pulses are "asynchronous" with the measurement times. Cullers' ground breaking analysis was restricted to the finite/synchronous category, whereas this paper examines all four cases and ultimately favors the more credible infinite/asynchronous assumption.

Finally, Cullers and I both recognized the need to modify the pulse detection algorithm to allow it to indicate the reception of a sequence of i pulses even if some of those pulses do not exceed the power threshold $T(i)$. This has the effect of lowering the probability of missing a potential ETI signal at the expense of a higher false-alarm rate. We agreed that for a given i, the number of pulses allowed to fall below $T(i)$ would be kept small enough to permit the period of the detected pulse train to be uniquely determined.

II. The Algorithm

As mentioned earlier, the SETI equipment uses a spectrum analyzer to generate a frequency-time matrix of received powers. The pulse detection algorithm investigates the hypothesis that embedded in that data record is a sequence of i periodically spaced pulses, where i is an unknown parameter that in general can be any integer between 1 and the number of time cells N. Because of the desire to process a given data record in real time, the two-dimensional array of received powers is soft quantized by tagging each frequency-time cell according to the largest power threshold exceeded in the preselected set $\{T(i)\}$.

To simplify the analysis, we will assume that a received pulse train does not drift in frequency during the observation interval, and focus on the operation of the detection algorithm on a single frequency channel. Furthermore, although the algorithm simultaneously searches for pulse trains with many values of $i \geq 1$, we will consider a particular value of i and compute the corresponding $T(i)$ that produces a desired false-alarm rate.

So the observation space of interest is a sequence of N spectral power measurements that have been hard quantized by a threshold $T(i)$. As stated earlier, we assume that the power in each pulse is largely contained within a single time cell (this is not meant to imply the synchronous restriction). Even within these constraints, there are still two important degrees of freedom to resolve—the phase and period of the received pulse train. The phase is defined by the integer $k \in [1, N]$, which

denotes the time cell containing the first pulse within the observation window. In the synchronous case, the period is the integer spacing $m \geq 1$ between cells containing consecutive pulses. However, in the asynchronous case, the period m is noninteger, so the second degree of freedom is defined by the integer spacing $\ell \cong (i-1)\,m$ between the cells containing the first and last received pulses. Depending on whether the pulse train is assumed to be finite or infinite, these degrees of freedom will have some constraints or boundary conditions. For the four cases of interest (e.g. infinite/synchronous), the domain of allowable degrees of freedom defines $g(i)$ *distinct* subsets of i cells within the N cell data record where the received pulses could be located. The boundary conditions and the parameters $g(i)$ are derived in the next two sections.

Consider a *particular* group of i cells that is a member of the subset of $g(i)$ potential pulse train locations. A very restrictive pulse detection algorithm might insist that the power levels in *all* i cells exceed $T(i)$, while the remaining $(N-i)$ cells fail the threshold test. While such an algorithm would have a low false-alarm rate, it would be at the expense of a higher probability of missing a received pulse train. A more reasonable criterion is to declare that a sequence of i periodically spaced pulses has been detected whenever *any* $(i-J)$ of them or more satisfy the threshold test, and allow up to a small number K of the other $(N-i)$ cells to exceed the power threshold erroneously due to thermal noise. Of course, J and K would be kept small enough to ensure unambiguous determinations of i and m, and to maintain a sufficiently low false-alarm rate.

To compute the false alarm probability P_{FA}, we assume that the N spectral power measurements represent internal system noise only. The power in each cell is then a central chi-square random variable with two degrees of freedom. If the cell powers and the threshold $T(i)$ are normalized by dividing each by the mean cell power, the probability that a given cell erroneously satisfies the threshold test is

$$p = e^{-T(i)} \tag{1}$$

Then, for the modified pulse detection algorithm described above,

$$P_{FA} = g(i) \sum_{j=0}^{J} \binom{i}{j} p^{i-j} (1-p)^{j} \sum_{k=0}^{K} \binom{N-i}{k} p^{k} (1-p)^{N-i-k} \tag{2}$$

If $p \ll 1$, P_{FA} will be dominated by the $j = J$, $k = 0$ terms, so that a good approximation that avoids having to select a particular K is

$$\begin{aligned} P_{FA} &\cong g(i) \binom{i}{J} p^{i-J} (1-p)^{N-i+J} \\ &= g(i) \binom{i}{J} e^{-(i-J)\,T(i)} \left[1 - e^{-T(i)}\right]^{N-i+J} \end{aligned} \tag{3}$$

In the next two sections, we will compute $g(i)$ according to whether the pulse train is assumed to be synchronous or asynchronous, and finite or infinite. In all four cases, the first degree of freedom represented by the integer location k of the first received pulse is trivially constrained by

$$1 \leq k \leq N \tag{4}$$

In the special case $i = 1$, only a single pulse is observed and m cannot be determined from the available data. Then there is only the single degree of freedom given by Eq. 4, and in all four cases,

$$g(1) = N \tag{5}$$

We shall now derive boundary conditions on the second degree of freedom, and compute $g(i)$ for $i \geq 2$.

III. Synchronous Case

Here the second degree of freedom is the integer period m. Since the last of the i pulses must lie within the N observed cells, we must have $k + (i-1)\,m \leq N$, or

$$m \leq \frac{N-k}{i-1}; \quad i \geq 2 \tag{6}$$

for both the finite and infinite cases. The infinite assumption further demands that the number of cells prior to the first pulse and following the last one within the span of N be strictly less than the period m: that is, $k, -N-k\ -(i-1)m + 1 \leq m$, or equivalently

$$m \geq k, \frac{N-k+1}{i} \tag{7}$$

In the finite/synchronous case previously analyzed by Cullers, the domain of (k, m) defined by Eqs. 4 and 6 is illustrated in Fig. 1. Every integer pair within this triangular domain corresponds to a distinct member of the $g(i)$ possible pulse train locations, so that

$$\begin{aligned} g(i) &= \sum_{m=1}^{\mu} [N-(i-1)m]; \quad \mu \equiv \left\lfloor \frac{N-1}{i-1} \right\rfloor \\ &= N\mu - \frac{1}{2}(i-1)\,\mu\,(\mu+1); \quad i \geq 2 \end{aligned} \tag{8}$$

where $\underline{x}$ denotes the integer part of x. As an approximation, if we ignore the requirement that μ be an integer and substitute $\mu \cong (N-1)/(i-1)$ into Eq. 8, we find that $g(i)$ reduces to the approximation

$$g(i) \cong \frac{(N-1)(N-i+2)}{2(i-1)}; \quad i \geq 2$$
$$\cong \frac{N^2}{2(i-1)}; \quad N >> 1, i \tag{9}$$

These are the same results obtained by Cullers in Ref. 1.

Note that the series summation of Eq. 8 looks like a numerical integration of the area of the triangular domain of (k, m) in Fig. 1. A loose approximation to $g(i)$ is simply the area of that triangle:

$$g(i) \cong \frac{(N-i)^2}{2(i-1)} \cong \frac{N^2}{2(i-1)}; \quad i \geq 2, N >> i \tag{10}$$

In the infinite/synchronous case, the domain of (k, m) must be modified to include the additional boundary conditions of Eq. 7, as illustrated in Fig. 2. Let $\overline{x}$ denote the smallest integer greater than or equal to x: then defining

$$\mu_1 \equiv \left\lfloor \frac{N+1}{i+1} \right\rfloor \quad \mu_2 \equiv \left\lfloor \frac{N}{i} \right\rfloor \quad \mu_3 \equiv \left\lfloor \frac{N-1}{i-1} \right\rfloor \tag{11}$$

allows us to write

$$g(i) = \sum_{m=\mu_1}^{\mu_2} [(i+1)m - N] + \sum_{m=\mu_2+1}^{\mu_3} [N - (i-1)m]$$
$$= N(\mu_1 - 2\mu_2 + \mu_3 - 1)$$
$$+ \frac{i}{2}(\mu_1 - \mu_1^2 + 2\mu_2 + 2\mu_2^2 - \mu_3 - \mu_3^2)$$
$$+ \frac{1}{2}(\mu_1 - \mu_1^2 + \mu_3 + \mu_3^2); \quad i \geq 2 \tag{12}$$

Ignoring the integer constraints in Eq. 11, and substituting the noninteger expressions for μ_1, μ_2, and μ_3 into Eq. 12 yields the approximation

$$g(i) \cong \frac{N^2 + i^3 - i^2 - i}{i(i^2-1)}; \quad i \geq 2$$
$$\cong \frac{N^2}{i(i^2-1)}; \quad N >> i \tag{13}$$

As a check, the area of the trapezoidal domain in Fig. 2 gives the approximation

$$g(i) \cong \frac{(N-i)^2}{i(i^2-1)} \cong \frac{N^2}{i(i^2-1)}; \quad i \geq 2, N >> i \tag{14}$$

IV. Asynchronous Case

Now the second degree of freedom is the integer spacing ℓ between the cells containing the first and last received pulses. The nominal or *observed* period is therefore

$$\hat{m} = \frac{\ell}{i-1} \cong m; \quad i \geq 2 \tag{15}$$

Assuming that the duration of each pulse is much smaller than the width of each time cell, the actual locations of these pulses can deviate from the centers of the cells containing them by up to half a cell width in either direction. Therefore, the true, noninteger period lies in the range

$$\frac{\ell - 1}{i-1} < m < \frac{\ell + 1}{i-1}$$
$$\Downarrow \tag{16}$$
$$|m - \hat{m}| < \frac{1}{i-1}$$

which becomes negligible for large i.

In both the finite and infinite cases, clearly $k + \ell \leq N$, or

$$\ell \leq N - k \tag{17}$$

Because of the uncertainty as to the true value of m, we shall use the *approximate* boundary modifications

$$k, \; N - k - \ell + 1 \lesssim \hat{m}$$

for the infinite case, which implies that

$$\ell \gtrsim (i-1)k, \left(\frac{i-1}{i}\right)(N - k + 1); \quad i \geq 2 \tag{18}$$

The domains for both sets of boundary conditions are illustrated in Figs. 3 and 4. Unlike the synchronous cases, there is not a one-to-one correspondence between integer pairs (k, ℓ) in these domains and distinct subsets of i cells containing the received pulses. Although the cell locations of the first and last pulses are fixed for a given (k, ℓ), because the pulse sequence is asynchronous with the time cells, each of the $(i-2)$ intermediate pulses can often occupy one of two adjacent cells. For example, if $i = 3$ and ℓ is an odd integer, $\hat{m}$ is a half-integer, and the middle pulse could lie in either the $[k + (\ell - 1)/2]^{\text{th}}$ cell or the $[k + (\ell + 1)/2]^{\text{th}}$ cell: under these conditions, a particular integer pair (k, ℓ) in the domain (with ℓ odd) corresponds to two distinct patterns of i cells. On the other hand, if $i = 3$ and ℓ is even, each integer pair represents a single pattern of i cells. If ℓ is equally likely to be even or odd, *on the average* each (k, ℓ) represents 3/2 distinct i-cell subsets of the N observations. Denoting the number of integer pairs within an asynchronous domain by $f(i)$, we can represent the average number of i-cell pulse location patterns by

$$g(i) \equiv c(i) f(i) \tag{19}$$

where $c(2) = 1$ and we have argued above that $c(3) = 3/2$. A more rigorous derivation of $c(i)$ is given in the Appendix; we show that

i	$c(i)$
3	1.5
4	3
5	5.25
6	13
7	17.5

There remains the computation of $f(i)$. In the finite case of Fig. 3,

$$f(i) = \sum_{\ell=1}^{N-1} (N - \ell) = \frac{1}{2} N(N-1); \quad i \geq 2$$

$$\cong \frac{N^2}{2}; \quad N >> 1 \tag{20}$$

which is *independent of i*. In the infinite case, remembering that the lower boundaries in the domain of Fig. 4 are approximate,

$$f(i) \cong \sum_{\ell=\lambda_1}^{\lambda_2} \left[\left(\frac{i+1}{i-1} \right) \ell - N \right] + \sum_{\ell=\lambda_2+1}^{N-1} (N - \ell)$$

$$= (\lambda_2 - \lambda_1 + 1) \left[\frac{1}{2} \left(\frac{i+1}{i-1} \right) (\lambda_2 + \lambda_1) - N \right]$$

$$+ \frac{1}{2} (N - \lambda_2)(N - \lambda_2 - 1); \quad i \geq 2 \tag{21a}$$

where

$$\lambda_1 \equiv \left\lceil \left(\frac{i-1}{i+1} \right) (N+1) \right\rceil$$

$$\lambda_2 \equiv \left\lfloor \left(\frac{i-1}{i} \right) N \right\rfloor \tag{21b}$$

Ignoring the integer restrictions on λ_1 and λ_2, Eq. 21 simplifies to

$$f(i) \cong \frac{N^2 + i}{i(i+1)}; \quad i \geq 2$$

$$\cong \frac{N^2}{i(i+1)}; \quad N >> i \tag{22}$$

V. Example

Suppose $N = 100$ and we want to determine a set of thresholds $\{T(i)\}$ such that $P_{FA} = 2 \times 10^{-12}$ independent of i. We will assume that the pulse detection algorithm is looking for infinite/asynchronous pulse trains, and we will allow $J = 1$ of the i pulses to fail the threshold test for $i \geq 4$, keeping $J = 0$ for smaller i. From Eqs. 3, 5, 19, and 22, we have

$$P_{FA} = N e^{-T(1)} \left[1 - e^{-T(1)} \right]^{N-1}; \quad i = 1$$

$$P_{FA} = c(i) \left[\frac{N^2 + i}{i(i+1)} \right] \binom{i}{J} e^{-(i-J)T(i)} \left[1 - e^{-T(i)} \right]^{N-i+J};$$

$$i \geq 2 \tag{23}$$

The resulting thresholds, normalized in terms of the mean cell power, are

i	$T(i)$	
1	31.5	$J = 0$
2	17.2	
3	11.4	
4	11.9	$J = 1$
5	9.0	
6	7.3	
7	6.1	

VI. Postscript

This work was recently presented at the SETI SWG meeting at Ames Research Center. It became evident from the audience's questions that the actual operation of the pulse detection algorithm using a superposition of thresholds $\{T(i): 1, 2, \cdots\}$ was not clear. To alleviate this problem, the synchronous example illustrated in Fig. 5 was used. The example considers a single data record of $N = 25$ time cells for an arbitrary frequency bin. The algorithm first searches for a single pulse exceeding the power threshold $T(1)$, then for two cell powers exceeding $T(2)$, then for three periodically spaced pulses exceeding $T(3)$, and so on. This is a special case of the algorithm described earlier with $J = 0$.

In the particular example of Fig. 5, there are no cell powers that exceed $T(1)$, only one exceeds $T(2)$, and, although three do exceed $T(3)$, they are not periodically spaced; so the algorithm does not see a sequence of i periodic pulses for $1 \leqslant i \leqslant 3$. However, six cell powers exceed $T(4)$, including the periodic sequence consisting of cells 4, 10, 16, and 22, so the algorithm flags that 4-cell subset.

References

1. Cullers, D. K., Oliver, B. M., Day, J. R., and Olsen, E., "Signal Recognition," in Appendix III of *1983 Report of the SETI Science Working Group*, edited by F. Drake, J. H. Wolfe, and C. L. Seeger. NASA/Ames Research Center, Moffett Field, California, February 1983.

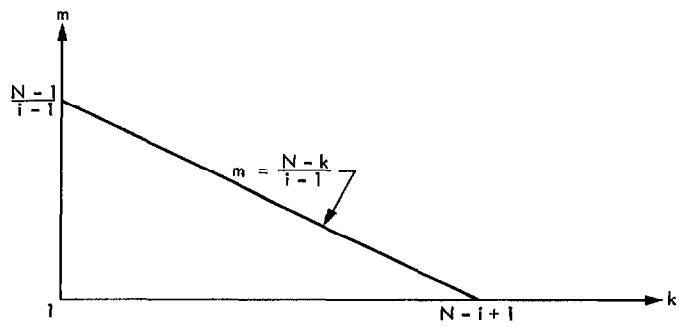

Fig. 1. Domain of (k, m) for finite/synchronous case, where $i \geq 2$

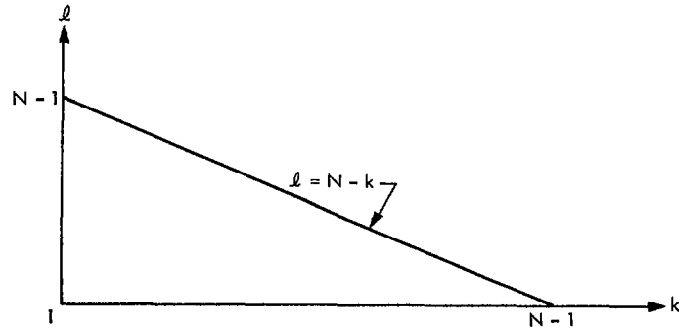

Fig. 3. Domain of (k, ℓ) for finite/asynchronous case, where $i \geq 2$

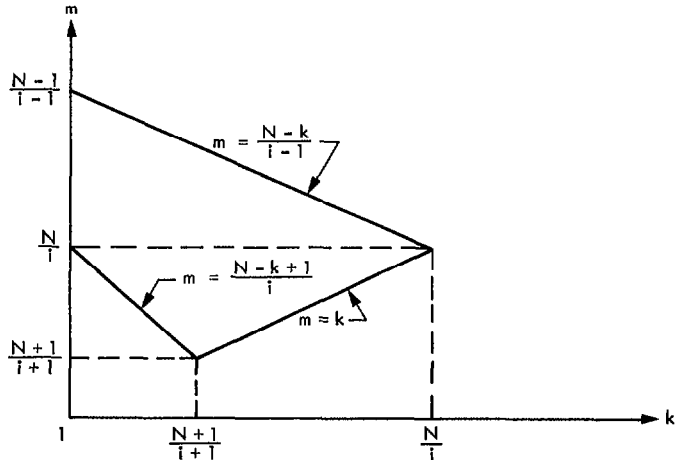

Fig. 2. Domain of (k, m) for infinite/synchronous case, where $i \geq 2$

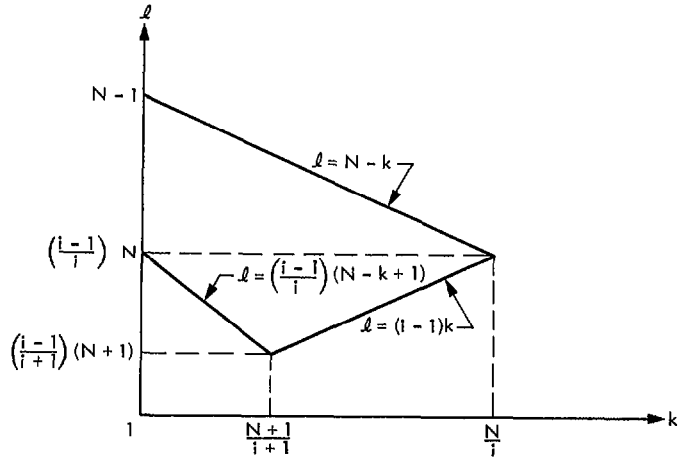

Fig. 4. Domain of (k, ℓ) for infinite/asynchronous case, where $i \geq 2$

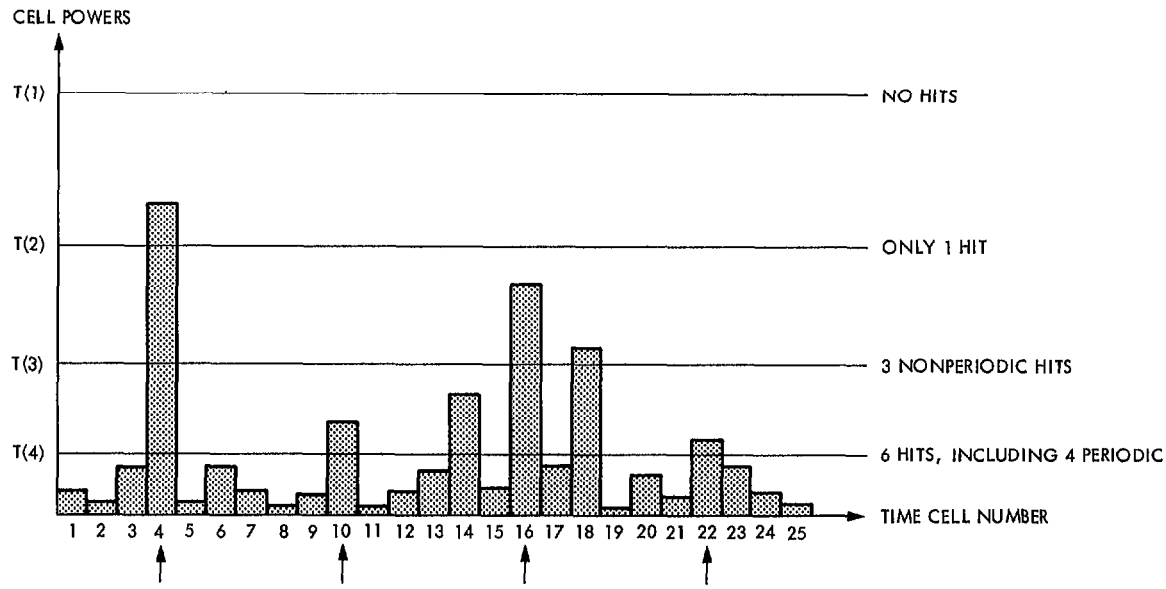

Fig. 5. Example of sequential investigation of hypothesis that a sequence of i periodic pulses is present in data record of $N = 25$ time cells, $i = 1, 2, \ldots$. The ($J = 0$) algorithm demands that i periodically spaced cell powers exceed $T(i)$. The synchronous case is assumed

Appendix

Computation of $c(i)$ for Asynchronous Pulse Trains

Consider a sequence of i periodic pulses received within a data record of N time cells. The duration of each pulse is assumed to be much smaller than a cell interval, so we can essentially regard it as occuring at a single point in time. Furthermore, all time measurements below are in time cell units, so that the normalized sample times are the integers $1, 2, \cdots, N$. In the asynchronous case, the pulse period m and the times of occurrence of the pulses $x_1, x_2, \cdots, x_i$ are noninteger. The j^{th} pulse is received in the y_j^{th} cell, where

$$x_j = y_j + \Delta_j; \quad |\Delta_j| < \frac{1}{2} \tag{A-1}$$

and y_j is integer. In Section IV, we defined the observed period (Eq. 15)

$$\hat{m} \equiv \frac{\ell}{i-1} = \frac{y_i - y_1}{i-1} \tag{A-2}$$

whereas the actual period is

$$m = \frac{x_i - x_1}{i-1} = \hat{m} + \frac{\Delta_i - \Delta_1}{i-1} \tag{A-3}$$

which satisfies Eq. 16.

For particular first and last observed pulse locations, y_1 and y_i, which fix $\ell \equiv y_i - y_1$, we want to investigate the range of observed intermediate pulse locations $y_2, y_3, \cdots, y_{i-1}$, for $i \geq 3$. The actual noninteger location of the j^{th} intermediate pulse $(2 \leq j \leq i-1)$ satisfies

$$\begin{aligned} x_j &= x_1 + (j-1)m \\ &= y_1 + \frac{i-j}{i-1}\Delta_1 + \left(\frac{j-1}{i-1}\right)(\ell + \Delta_1) \end{aligned} \tag{A-4}$$

If we denote

$$\ell_0 \equiv \left\lfloor \frac{\ell}{i-1} \right\rfloor$$

and $\ell_1 \equiv \ell \bmod (i-1)$, then $\ell = \ell_0 (i-1) + \ell_1$, where ℓ_0 and ℓ_1 are integers and $0 \leq \ell_1 \leq i-2$. In the analysis that follows, we will assume that ℓ_1 is uniformly likely to assume any value within its range. We can express Eq. A-4 as

$$x_j = \underbrace{y_1 + \ell_0(j-1)}_{\text{integer}} + \underbrace{\left(\frac{i-j}{i-1}\right)\Delta_1 + \left(\frac{j-1}{i-1}\right)(\ell_1 + \Delta_i)}_{\text{noninteger, } z_j} \tag{A-5}$$

Since y_j is the integer closest to x_j, the range of z_j determines the number of possible y_j's. Let $\vec{y} \equiv (y_1, y_2, \cdots, y_i)$ and D denote the number of distinct $\vec{y}$'s consistent with the given values of i, y_1, y_i. Then D equals the number of possible y_2's times the number of possible y_3's times $\cdots$ times the number of possible y_{i-1}'s, and

$$c(i) = E[D] \tag{A-6}$$

where the expectation is over the discrete uniform random variable ℓ_1. Since $|\Delta_1|, |\Delta_i| < 1/2$, and Δ_1 and Δ_i are independent parameters,

$$\left| \left(\frac{i-j}{i-1}\right)\Delta_1 + \left(\frac{j-1}{i-1}\right)\Delta_i \right| < \frac{1}{2}$$

$$\Downarrow$$

$$\left| z_j - \left(\frac{j-1}{i-i}\right)\ell_1 \right| < \frac{1}{2} \tag{A-7}$$

If

$$\left(\frac{i-1}{i-1}\right)\ell_1$$

is an integer, which is always true when $\ell_1 = 0$, then there is only one possible value of y_j:

$$\begin{aligned} y_j &= y_1 + \ell_0 (j-1) + \left(\frac{j-1}{i-1}\right)\ell_1 \\ &= y_1 + \left(\frac{j-1}{i-1}\right)\ell \end{aligned} \tag{A-8}$$

However, if

$$\left(\frac{j-1}{i-1}\right) \ell_1$$

is noninteger, then y_j can have one of two possible values:

$$\begin{aligned} y_j &= y_1 + \ell_0 (j-1) + \left\lfloor \left(\frac{j-1}{i-1}\right) \ell_1 \right\rfloor \\ y_j &= y_1 + \ell_0 (j-1) + \left\lfloor \left(\frac{j-1}{i-1}\right) \ell_1 \right\rfloor + 1 \end{aligned} \qquad \text{(A-9)}$$

So, for a given i and ℓ_1, D is simply 2 raised to the number of noninteger members of the set

$$\left\{ \left(\frac{j-1}{i-1}\right) \ell_1 \; ; 2 \leqslant j \leqslant i-1 \right\};$$

in particular

$$1 \leqslant D \leqslant 2^{i-2} \qquad \text{(A-10)}$$

Table A-1 illustrates the calculation of $c(i)$ for $i \geqslant 3$.

Table A-I. Calculation of parameter c(*i*)

i	ϱ_1	j	$\left(\frac{j-1}{i-1}\right)\varrho_1$	D	$c(i)$
3	0	2	0	1	1.5
	1	2	noninteger	2	
4	0	2	0	1	3
		3	0		
	1	2	noninteger	4	
		3	noninteger		
	2	2	noninteger	4	
		3	noninteger		
5	0	2	0	1	5.25
		3	0		
		4	0		
	1	2	noninteger	8	
		3	noninteger		
		4	noninteger		
	2	2	noninteger	4	
		3	1		
		4	noninteger		
	3	2	noninteger	8	
		3	noninteger		
		4	noninteger		